

**Fermi National Accelerator Laboratory**

**FERMILAB-Pub-97/105-E**

**E791**

**Asymmetries Between the Production of  $D_s^-$  and  $D_s^+$  Mesons from  
500 GeV/c  $\pi^-$  Nucleon Interaction as Functions of  $x_F$  and  $p_t$ <sup>2</sup>**

E.M. Aitala et al.

The E791 Collaboration

*Fermi National Accelerator Laboratory  
P.O. Box 500, Batavia, Illinois 60510*

July 1997

Submitted to *Physics Letters B*

## **Disclaimer**

*This report was prepared as an account of work sponsored by an agency of the United States Government. Neither the United States Government nor any agency thereof, nor any of their employees, makes any warranty, expressed or implied, or assumes any legal liability or responsibility for the accuracy, completeness, or usefulness of any information, apparatus, product, or process disclosed, or represents that its use would not infringe privately owned rights. Reference herein to any specific commercial product, process, or service by trade name, trademark, manufacturer, or otherwise, does not necessarily constitute or imply its endorsement, recommendation, or favoring by the United States Government or any agency thereof. The views and opinions of authors expressed herein do not necessarily state or reflect those of the United States Government or any agency thereof.*

## **Distribution**

*Approved for public release; further dissemination unlimited.*

**Asymmetries Between the Production of  $D_s^-$  and  $D_s^+$   
Mesons from 500 GeV/c  $\pi^-$  Nucleon Interaction as Functions  
of  $x_F$  and  $p_t^2$**

E. M. Aitala,<sup>9</sup> S. Amato,<sup>1</sup> J. C. Anjos,<sup>1</sup> J. A. Appel,<sup>5</sup> D. Ashery,<sup>15</sup> S. Banerjee,<sup>5</sup>  
I. Bediaga,<sup>1</sup> G. Blaylock,<sup>8</sup> S. B. Bracker,<sup>16</sup> P. R. Burchat,<sup>14</sup> R. A. Burnstein,<sup>6</sup>  
T. Carter,<sup>5</sup> H. S. Carvalho,<sup>1</sup> N. K. Coptý,<sup>13</sup> L. M. Cremaldi,<sup>9</sup> C. Darling,<sup>19</sup>  
K. Denisenko,<sup>5</sup> A. Fernandez,<sup>12</sup> P. Gagnon,<sup>2</sup> C. Gobel,<sup>1</sup> K. Gounder,<sup>9</sup>  
A. M. Halling,<sup>5</sup> G. Herrera,<sup>4</sup> G. Hurvits,<sup>15</sup> C. James,<sup>5</sup> P. A. Kasper,<sup>6</sup> S. Kwan,<sup>5</sup>  
D. C. Langs,<sup>11</sup> J. Leslie,<sup>2</sup> B. Lundberg,<sup>5</sup> S. MayTal-Beck,<sup>15</sup> B. Meadows,<sup>3</sup>  
J. R. T. de Mello Neto,<sup>1</sup> D. Mihalcea,<sup>7</sup> R. H. Milburn,<sup>17</sup> J. M. de Miranda,<sup>1</sup>  
A. Napier,<sup>17</sup> A. Nguyen,<sup>7</sup> A. B. d'Oliveira,<sup>12</sup> K. O'Shaughnessy,<sup>2</sup> K. C. Peng,<sup>6</sup>  
L. P. Perera,<sup>3</sup> M. V. Purohit,<sup>13</sup> B. Quinn,<sup>8</sup> S. Radeztsky,<sup>18</sup> A. Rafatian,<sup>9</sup>  
N. W. Reay,<sup>7</sup> J. J. Reidy,<sup>9</sup> A. C. dos Reis,<sup>1</sup> H. A. Rubin,<sup>6</sup> A. K. S. Santha,<sup>3</sup>  
A. F. S. Santoro,<sup>1</sup> A. J. Schwartz,<sup>11</sup> M. Sheaff,<sup>18</sup> R. A. Sidwell,<sup>7</sup> A. J. Slaughter,<sup>19</sup>  
M. D. Sokoloff,<sup>3</sup> N. R. Stanton,<sup>7</sup> K. Stenson,<sup>18</sup> D. J. Summers,<sup>9</sup> S. Takach,<sup>19</sup>  
K. Thorne,<sup>5</sup> A. K. Tripathi,<sup>10</sup> S. Watanabe,<sup>18</sup> R. Weiss-Babai,<sup>15</sup> J. Wiener,<sup>11</sup>  
N. Witcheý,<sup>7</sup> E. Wolin,<sup>19</sup> D. Yi,<sup>9</sup> S. Yoshida,<sup>7</sup> R. Zaliznyak,<sup>14</sup> and C. Zhang<sup>7</sup>

(Fermilab E791 Collaboration)

<sup>1</sup> *Centro Brasileiro de Pesquisas Físicas, Rio de Janeiro, Brazil*

<sup>2</sup> *University of California, Santa Cruz, California 95064*

<sup>3</sup> *University of Cincinnati, Cincinnati, Ohio 45221*

<sup>4</sup> *CINVESTAV, Mexico*

<sup>5</sup> *Fermilab, Batavia, Illinois 60510*

<sup>6</sup> *Illinois Institute of Technology, Chicago, Illinois 60616*

<sup>7</sup> *Kansas State University, Manhattan, Kansas 66506*

<sup>8</sup> *University of Massachusetts, Amherst, Massachusetts 01003*

<sup>9</sup> *University of Mississippi, University, Mississippi 38677*

<sup>10</sup> *The Ohio State University, Columbus, Ohio 43210*

<sup>11</sup> *Princeton University, Princeton, New Jersey 08544*

<sup>12</sup> *Universidad Autonoma de Puebla, Mexico*

<sup>13</sup> *University of South Carolina, Columbia, South Carolina 29208*

<sup>14</sup> *Stanford University, Stanford, California 94305*

<sup>15</sup> *Tel Aviv University, Tel Aviv, Israel*

<sup>16</sup> *317 Belsize Drive, Toronto, Canada*

<sup>17</sup> *Tufts University, Medford, Massachusetts 02155*

<sup>18</sup> *University of Wisconsin, Madison, Wisconsin 53706*

<sup>19</sup> *Yale University, New Haven, Connecticut 06511*

(July 11, 1997)

## Abstract

We present measurements of the production of  $D_s^-$  mesons relative to  $D_s^+$  mesons as functions of  $x_F$  and of  $p_t^2$  for a sample of 2445  $D_s$  decays to  $\phi\pi$ . The  $D_s$  mesons were produced in Fermilab experiment E791 with 500 GeV/c  $\pi^-$  mesons incident on one platinum and four carbon foil targets. The acceptance-corrected integrated asymmetry in the  $x_F$  range  $-0.1$  to  $0.5$  for  $D_s^\mp$  mesons is  $0.032 \pm 0.022 \pm 0.022$ , consistent with no net asymmetry. We compare the results as functions of  $x_F$  and  $p_t^2$  to predictions and to the large production asymmetry observed for  $D^\pm$  mesons in the same experiment. These comparisons support the hypothesis that production asymmetries come from the fragmentation process and not from the charm quark production itself.

Previous studies of charm particle production in hadron beams [1–9] have shown large enhancements in the forward production of charm particles that contain a quark or di-quark in common with the beam (leading particles) relative to those that do not (non-leading particles). Neither leading-order nor next-to-leading-order perturbative QCD calculations of charm quark production can account for the observed asymmetries [10,11]. The phenomenon is due either to unexpected contributions to charm quark production or to features of the hadronization process.

Three classes of models have been proposed to account for hadronization in the beam fragmentation region: coalescence of produced charm quarks with valence quarks or diquarks from the beam [12–14], coalescence of charm and valence quarks when both originate in the beam particle [15,16], and string fragmentation as implemented in the Lund Model of the PYTHIA Monte Carlo program [17] and by Piskounova [18]. All these models involve a mechanism of attachment between the produced charm quarks and the valence quarks in the beam, and include a varying amount of actual coalescence. This coalescence is the dominant mechanism for the leading particle effect in the first two classes of models. They include no mechanism which will lead to a significant production asymmetry between particles except when one of them has a quark in common with the beam and the other does not. Since the probability of coalescence between two quarks is larger when they have similar velocities, the production asymmetry between leading and nonleading charm mesons is expected to grow larger with increasing  $x_F$  and smaller with increasing  $p_t^2$ . While  $D^\pm$  data from Fermilab experiment E791 do show the expected increase in asymmetry with increasing  $x_F$ , they do not support the prediction of decreasing asymmetry with increasing  $p_t^2$  [7].

In string fragmentation models, specifically the PYTHIA/LUND implementation, a produced charm quark is always initially connected via color strings to valence quarks or diquarks in the beam and the target. A leading particle can be produced by a meson beam in cases where the string attaches a charm quark to a beam anti-quark and/or an anticharm quark to a beam quark. Some fraction of the time, the

string invariant mass is too small to allow the production of a quark-antiquark pair, and the process reduces to that of final state coalescence, with the same general features. However, in most cases additional  $q\bar{q}$  pairs are produced in the evolution of the strings. The string fragmentation model predicts an asymmetry even at relatively small values of  $x_F$ . This asymmetry is predicted to be relatively flat as a function of  $p_t^2$ , consistent with E791 measurements [7]. String fragmentation also allows for a possible asymmetry in cases where there is no quark in common with the beam, if one of the quarks is produced in the string fragmentation.

For the nearly pure  $\pi^-(\bar{u}d)$  beam [19] in Fermilab experiment E791 [23],  $D^-(\bar{c}d)$  is a leading particle and  $D^+(c\bar{d})$  is the corresponding nonleading particle. We have previously reported a significant  $D^\mp$  production asymmetry, increasing with  $x_F$  and relatively flat in  $p_t^2$ , and well represented by a modified version of the PYTHIA/LUND Monte Carlo [7]. In contrast,  $D_s^+(c\bar{s})$  and  $D_s^-(\bar{c}s)$  mesons do not share any valence quark type with the pion beam. There should thus be no asymmetry between  $D_s^-$  and  $D_s^+$  production if the effect is due to coalescence. The limited  $D_s$  sample sizes in previous experiments did not allow a detailed measurement of the production asymmetry for  $D_s$  mesons [3,22]. Indeed, no  $D_s$  asymmetry data has been reported for pion-induced production. We report the first results on the  $D_s$  production asymmetry in pion-nucleon collisions, and with sufficient data to study the asymmetry as functions of  $x_F$  and of  $p_t^2$ .

The E791 spectrometer [23] had 23 silicon microstrip detector planes (SMD's); six upstream of the target foils, seventeen downstream, to measure charged particle trajectories. This SMD system allows precise measurement of the position of the charm production vertex (primary vertex) and charm decay vertex (secondary vertex). Two magnets, together with the downstream SMDs, 35 drift chamber planes, and two proportional wire chamber planes, provided momentum measurement. Particle identification of pions, kaons, and protons was obtained with two segmented, threshold Čerenkov counters. The total E791 recorded data sample is  $2 \times 10^{10}$  500 GeV/ $c$   $\pi^-$  nucleon interactions, which satisfied a loose requirement on the total transverse en-

ergy deposited in the calorimeter, assuming that particles originate at the target foils. After data reconstruction, only those interactions in which one or more decay vertex candidates were detected were kept for further analysis.

From the above sample, charm meson decays to  $\phi\pi$  were sought by starting with candidate  $\phi \rightarrow K^+K^-$  decays. The  $\phi$  selection began with combinations of two oppositely charged, well-reconstructed tracks, at least one of which was identified as a kaon by the Čerenkov counters. The combination was retained as a  $\phi$  candidate if the invariant mass of the two tracks, assumed to be kaons, was within 10 MeV/ $c^2$  of the  $\phi$  mass (1.0194 GeV/ $c^2$ ). For each  $\phi$  candidate, a third track, assumed to be a pion, was sought for which the invariant mass of the three tracks, assumed to be  $KK\pi$ , was within a mass window 1.79 - 2.05 GeV/ $c^2$ , which includes both the  $D_s$  and the  $D^\pm$  masses. A fit to the point of intersection of the three tracks was then performed.

To further distinguish charm meson decays from background, additional selection criteria were applied to each secondary vertex candidate. The values of the selection criteria were chosen to maximize the statistical significance ( $N_s/\sqrt{(N_s + N_b)}$ ) for each  $x_F$  bin, where  $N_s$  is the number of  $D_s$  signal events and  $N_b$  is the number of background events under the  $D_s$  mass peak. The signal is represented by fully simulated  $D_s$  events generated by the PYTHIA Monte Carlo and the background is E791 data for which the candidate mass is in the sideband of the  $D_s$  peak, but outside the  $D^+$  signal region. For most of the  $x_F$  range, typical cuts are as follows. The longitudinal separation between the primary and secondary vertices was required to be more than 10 times the experimental resolution for the measured separation. The impact parameter of the reconstructed momentum vector of the  $D_s$  candidate with respect to the primary vertex was required to be less than 40 microns. The ratio of the distances of closest approach to the secondary and primary vertices were computed for each of the three decay tracks. The product of the three ratios was required to be less than 0.006. This means that in most cases the tracks that make the secondary vertex should be significantly closer to the secondary vertex than to the primary vertex.

It was required that no track in the event, except the three making the secondary vertex, pass within 10 microns of the secondary vertex.

Figure 1 shows the  $K^+K^-\pi^+$  and  $K^+K^-\pi^-$  invariant mass distributions after the above selection criteria are applied. A fit with two Gaussian curves and a linear background applied to the combined spectrum yields  $2445 \pm 60 D_s^\pm$  mesons and  $1449 \pm 55 D^\pm$  mesons. Fits to the individual spectra yield  $1188 \pm 41 D_s^+$  mesons,  $1257 \pm 42 D_s^-$  mesons,  $638 \pm 37 D^+$  mesons and  $811 \pm 40 D^-$  mesons. These uncorrected data show a clear excess of  $D^-$  mesons over  $D^+$  mesons, consistent with the earlier measurement by this collaboration for the more copious decay  $D^\pm \rightarrow K^\mp \pi^\pm \pi^\pm$  [7], but show no statistically significant asymmetry in the numbers of  $D_s^-$  and  $D_s^+$  mesons.

In order to study the asymmetry in the production of  $D_s^\pm$  mesons,  $K^+K^-\pi$  invariant mass plots were made for particular ranges of  $x_F$  and  $p_t^2$ . The yields of  $D_s^+$  and  $D_s^-$  mesons were then measured by fitting the peaks in the mass plots to Gaussian curves of fixed width and mean plus a linear background, and then integrating the area under the Gaussian curves. The evolution of the width of the Gaussian curves with  $x_F$  and  $p_t^2$  was determined from Monte Carlo simulation, and is the same for both charge states.

An asymmetry parameter  $A$  for  $D_s$  production is defined as

$$A \equiv \frac{N_{D_s^-} - N_{D_s^+}}{N_{D_s^-} + N_{D_s^+}}$$

Here,  $N_{D_s^-}$  is the number of negatively charged  $D_s$  mesons and  $N_{D_s^+}$  is the number of positively charged  $D_s$  mesons produced in a particular bin of  $x_F$  or  $p_t^2$ .

From studies using our complete Monte Carlo simulation, we find that our acceptance, which includes the geometrical acceptance as well as the reconstruction efficiency, falls off rapidly at high  $x_F$ . This inefficiency at high  $x_F$  increased with time during the data taking period. This was mainly due to beam effects which caused a cumulative local loss of efficiency in the drift chambers. A correction ranging from  $-6\%$  to  $+12\%$  was applied bin-by-bin for the difference between the acceptances of positive and negative  $D_s$  mesons. Residual uncertainties in this correction are treated

as systematic errors and are taken from reference [7], using the r.m.s. spread of four Monte Carlo simulations representing different time periods during the data taking.

A second source of systematic uncertainty is due to  $D_s$  mesons produced by the 2.5%  $K^-(\bar{u}s)$  content of the incident beam, for which the integrated asymmetry  $A$  is measured by E769, at 250 GeV/ $c$  beam energy, to be  $0.25 \pm 0.11$  [6]. No correction to the asymmetry is applied, but we assign a systematic error of 0.006 in the  $x_F$  range  $(-0.1$  to  $0.3)$  and 0.015 in the  $x_F$  range  $(0.3-0.5)$  to account for this source of systematic uncertainty. The increase in systematic error at larger  $x_F$  accounts for greater uncertainty in the  $K^-$  contribution in the forward direction.

The acceptance-corrected production asymmetry for  $D_s$  mesons in the  $x_F$  range  $-0.1$  to  $0.5$  is  $0.032 \pm 0.022 \pm 0.022$ , consistent with no net asymmetry. Here the first error is the statistical error and the second error is the systematic error from the sources described above.

The acceptance-corrected asymmetries as functions of  $x_F$  and  $p_t^2$  are shown in Tables I and II and in Figures 2 to 5. The asymmetries predicted by a tuned version of the PYTHIA/LUND Monte Carlo [20] are also shown in Figures 2 and 4 for comparison to the measured asymmetries. In this version of PYTHIA, parameters such as the mass of the charm quark and the intrinsic transverse momentum of the partons have been tuned so that the asymmetry of the Monte Carlo sample matches the asymmetry for the  $D^+ \rightarrow K\pi\pi$  using E791 data [7]. While E791 data are consistent with the PYTHIA model, a better  $\chi^2$  is obtained for the hypothesis of  $A=0$ . In Figure 3 we compare  $D_s$  and  $D^\pm$  asymmetries as a function of  $x_F$  measured using E791 data. The  $D^\pm$  data are from a high statistics measurement using the decay mode  $D^+ \rightarrow K\pi\pi$  [7]. The production asymmetry is larger for  $D^\pm$  mesons than for  $D_s$  mesons for all  $x_F$ . Figure 4 shows the  $D_s$  asymmetry as a function of  $p_t^2$  for E791 data and for the PYTHIA simulation mentioned above. The measured asymmetry is consistent with zero in all bins, but is also described well by the PYTHIA curve. Figure 5 shows a comparison of the measured  $D_s$  and the  $D^\pm$  asymmetries as a function of  $p_t^2$ . An intrinsic charm model predicts zero asymmetry for  $D_s$  production at

all  $x_F$  and  $p_t^2$  [15].

In summary, we have observed both  $D^\pm$  and  $D_s^\pm$  decays in the same apparatus and find a net production asymmetry only for the  $D^\pm$ . We find that the  $D_s$  asymmetry is consistent with zero in each bin of  $x_F$  and  $p_t^2$  in the ranges covered by E791. Since the beam used in experiment E791 contains almost no strange particles and the  $D_s$  asymmetry is consistent with zero, it can be concluded that the asymmetry seen in the  $D^\pm$  mesons is not likely to come from any asymmetry in the production of the charm quarks themselves, but originates in the hadronization process.

We gratefully acknowledge the assistance of the staffs of Fermilab and of all the participating institutions. This research was supported by the Brazilian Conselho Nacional de Desenvolvimento Científico e Tecnológico, CONACyT (Mexico), the Israeli Academy of Sciences and Humanities, the U.S. Department of Energy, the U.S.-Israel Binational Science Foundation and the U.S. National Science Foundation. Fermilab is operated by the Universities Research Association, Inc., under contract with the United States Department of Energy.

## REFERENCES

- [1] E595 Collaboration, J.L. Ritchie *et al.*, Phys. Lett. **B138**, 213 (1984).
- [2] NA27 Collaboration, M. Aguilar-Benitez *et al.*, Phys. Lett. **B161**, 400 (1985).
- [3] NA32 Collaboration, S. Barlag *et al.*, Z. Phys. **C49**, 555 (1991).
- [4] WA82 Collaboration, M. Adamovich *et al.*, Phys. Lett. **B305**, 402 (1993).
- [5] E769 Collaboration, G.A. Alves *et al.*, Phys. Rev. Lett. **72**, 812 (1994).
- [6] E769 Collaboration, G.A. Alves *et al.*, Phys. Rev. Lett. **77**, 2388 (1996).
- [7] E791 Collaboration, E.M. Aitala *et al.*, Phys. Lett. **B371**, 157 (1996).
- [8] WA89 Collaboration, R. Werding, Proceedings XXVII Int. Conf. on High Energy Physics, Glasgow, U.K., 20-27 July, 1994, p. 1023.
- [9] Beatrice Collaboration, M. Adamovich *et al.*, CERN Preprint CERN-PPE/96-180 (1996).
- [10] P. Nason, S. Dawson and R.K. Ellis, Nucl. Phys. **B327**, 49 (1989).
- [11] S. Frixione *et al.*, Nucl. Phys. **B431**, 453 (1994).
- [12] B.L. Combridge, Nucl. Phys. **B151**, 429 (1979).
- [13] V. Barger, F. Halzen, and W.Y. Keung, Phys. Rev. **D25**, 112 (1982).
- [14] P. Mazzanti and S. Wada, Phys. Rev. **D26**, 602 (1982).
- [15] R. Vogt, Nucl. Phys. **B478**, 311 (1996).
- [16] R.C. Hwa, Phys. Rev. **D51**, 85 (1995).
- [17] H.-U. Bengtsson and T. Sjöstrand, Comp. Phys. Comm. **46**, 43 (1987).
- [18] O.I. Piskounova, Nucl. Phys Proc. Suppl. **50**, 179 (1996).
- [19] A. Malensek, private communication.

- [20] Specific parameters changed in the PYTHIA Monte Carlo (version 5.7 with version 7.3 of JETSET) were PMAS(4.1) (the  $c$  quark mass in  $\text{GeV}/c^2$ ) changed from 1.35 to 1.7, PARP(91) (the average  $k_t^2$  in  $(\text{GeV}/c)^2$ ) increased from 0.44 to 1.0, PARP(93) (the maximum allowable  $k_t$  in  $(\text{GeV}/c)$ ) increased from 2.0 to 5.0, and MSTP(92) (the remnant quark-diquark energy splitting function) changed from 4 to 3.
- [21] S.J. Brodsky *et al.*, Phys. Lett. **93B**, 451 (1980); R. Vogt and S.J. Brodsky, Nucl. Phys. **B 438** 261 (1995).
- [22] E769 Collaboration, G.A. Alves *et al.*, Phys. Rev. Lett. **77**, 2392 (1996).
- [23] J.A. Appel, Ann. Rev. Nucl. Part. Sci. **42**, 367 (1992) and references therein; D.J. Summers *et al.*, Proceedings of the  $XXVII^{th}$  Rencontre de Moriond, Electroweak Interactions and Unified Theories, Les Arcs, France (15-22) March 1992, 417; S. Amato *et al.*, Nucl. Instr. Methods A, **324**, 535 (1993).

TABLE I.  $D_s$  production asymmetry as a function of  $x_F$  from E791 data, integrated over the  $p_t^2$  range 0 to 10  $(GeV/c)^2$ . The first error is statistical and the second systematic.

$x_F$	$D_s$ asymmetry A
-0.1 - 0.0	$0.015 \pm 0.054 \pm 0.023$
0.0 - 0.05	$-0.002 \pm 0.045 \pm 0.007$
0.05 - 0.1	$0.001 \pm 0.047 \pm 0.020$
0.1 - 0.2	$0.020 \pm 0.042 \pm 0.027$
0.2 - 0.25	$0.080 \pm 0.091 \pm 0.018$
0.25 - 0.3	$0.083 \pm 0.125 \pm 0.036$
0.3 - 0.4	$0.104 \pm 0.140 \pm 0.075$
0.4 - 0.5	$0.149 \pm 0.252 \pm 0.105$

TABLE II.  $D_s$  production asymmetry as a function of  $p_t^2$  from E791 data, integrated over the  $x_F$  range -0.1 to 0.5. The first error is statistical and the second systematic.

$p_t^2 (GeV/c)^2$	$D_s$ asymmetry A
0.0 - 1.0	$-0.016 \pm 0.035 \pm 0.013$
1.0 - 2.0	$0.036 \pm 0.043 \pm 0.036$
2.0 - 3.0	$0.089 \pm 0.052 \pm 0.056$
3.0 - 4.0	$0.081 \pm 0.056 \pm 0.089$
4.0 - 7.0	$0.032 \pm 0.053 \pm 0.078$
7.0 - 10.0	$-0.077 \pm 0.053 \pm 0.068$

# FIGURES

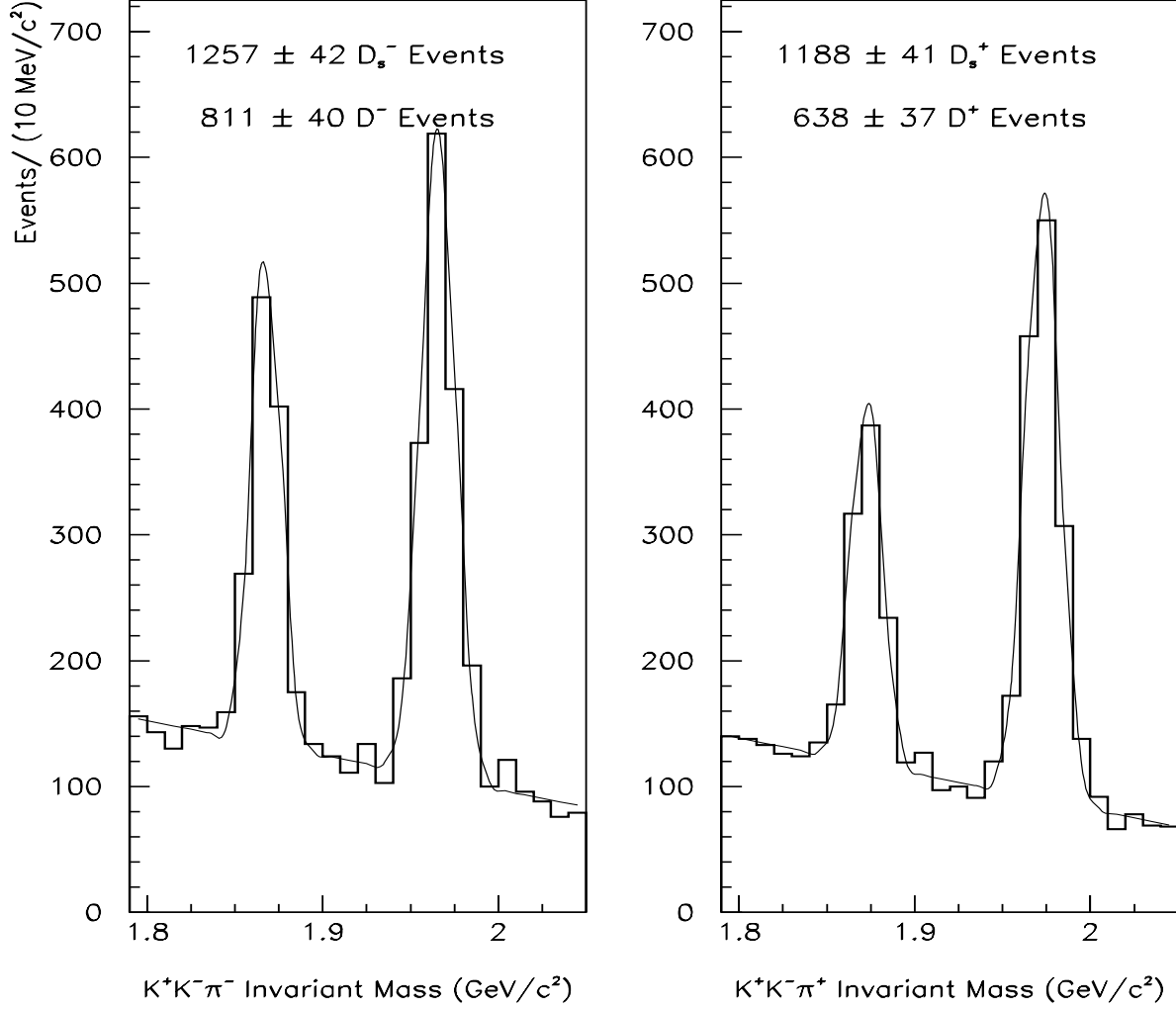


FIG. 1.  $K^+K^-\pi^+$  and  $K^+K^-\pi^-$  invariant mass plots.

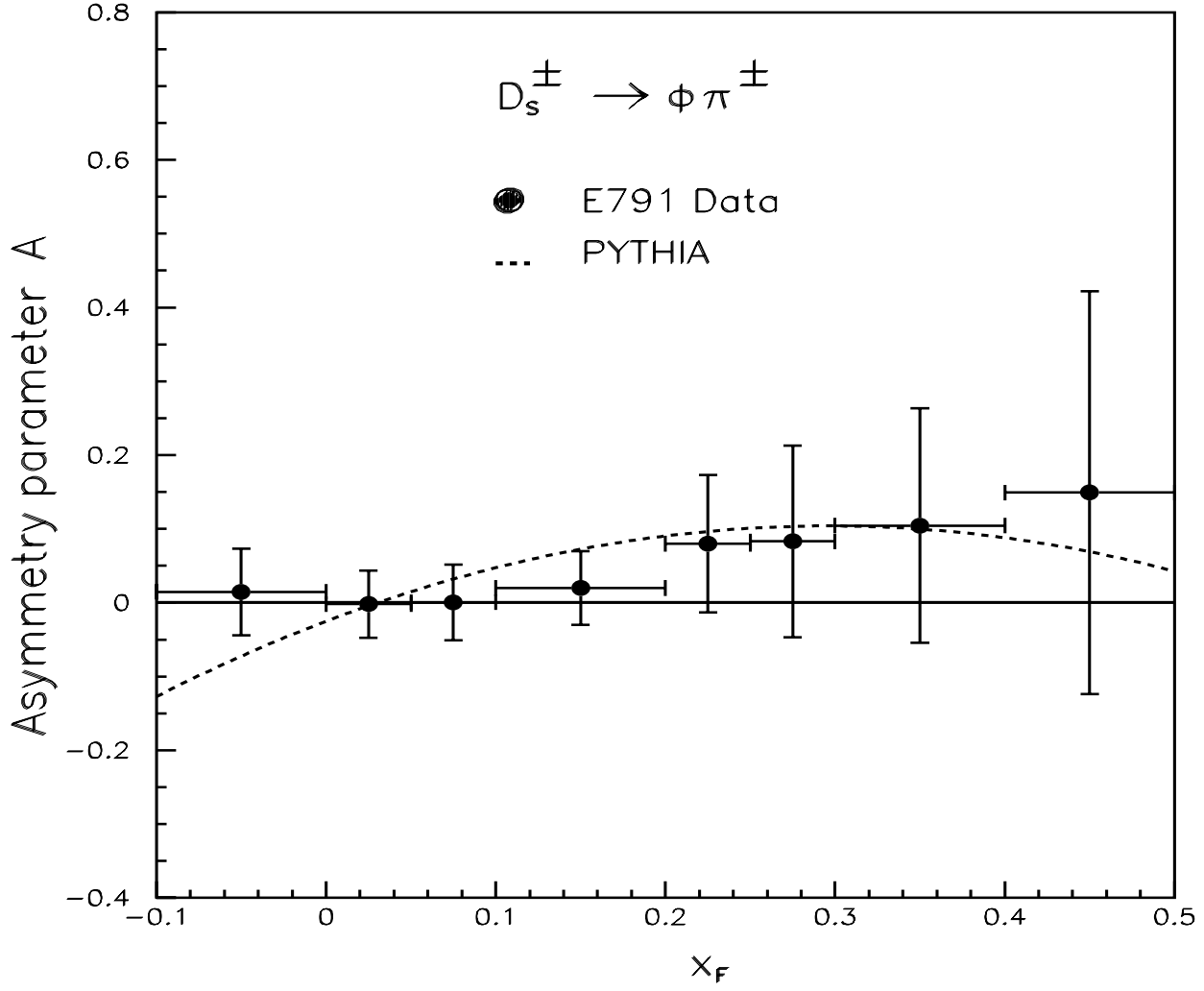


FIG. 2. Comparison of the measured  $D_s$  production asymmetry as a function of  $x_F$ , and the predictions (dashed line) of the tuned PYTHIA Monte Carlo described in the text. The acceptance corrected data are integrated over the  $p_t^2$  interval (1-10)  $(GeV/c)^2$ .

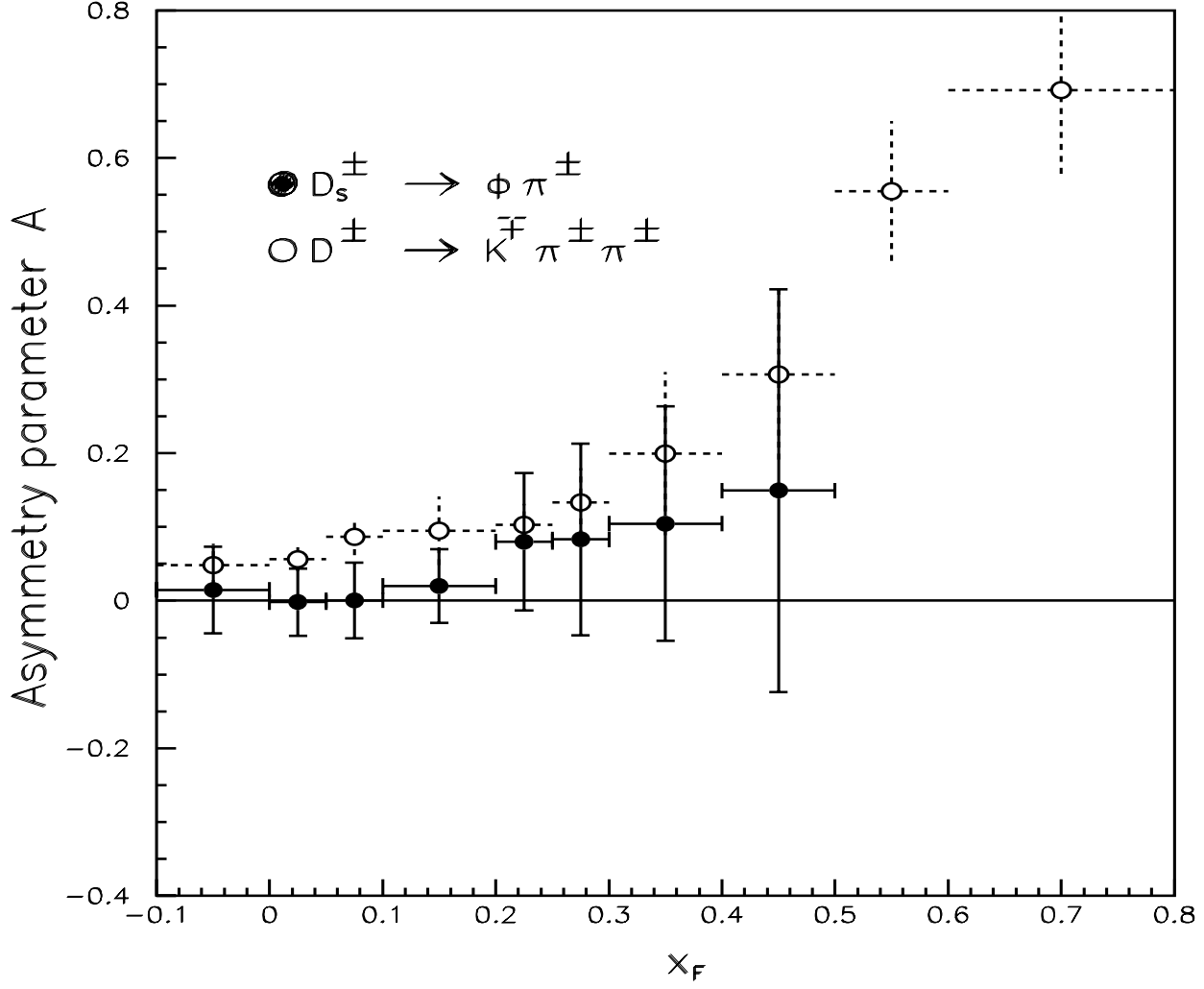


FIG. 3. Comparison of the  $D_s$  (solid circles) and  $D^+$  (open circles) production asymmetries measured by this experiment, as a function of  $x_F$ . The data are integrated over the  $p_t^2$  interval (1-10)  $(\text{GeV}/c)^2$ .

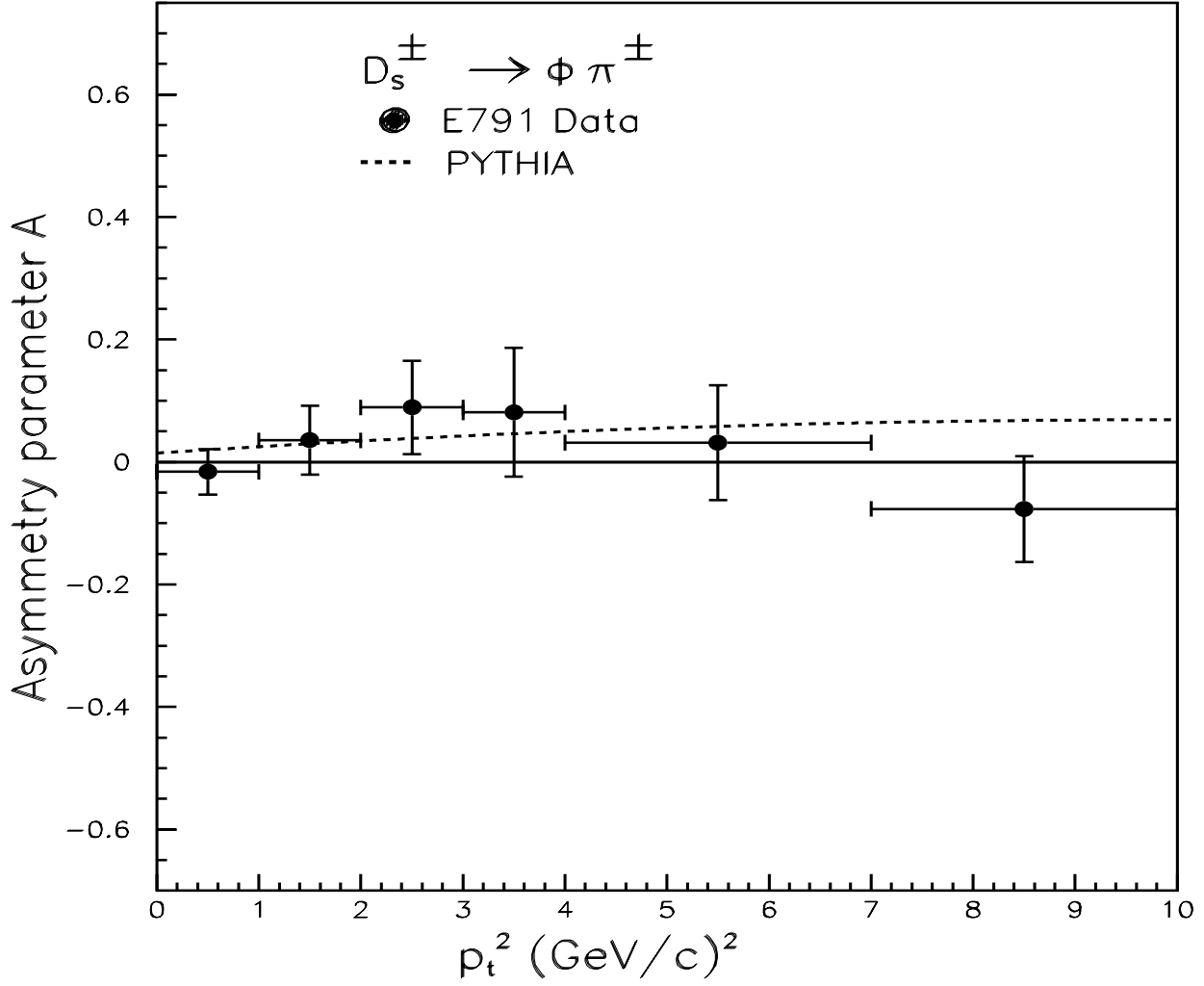


FIG. 4. Comparison of the measured  $D_s$  production asymmetry  $A$  (points with error bars), as a function of  $p_t^2$ , and the prediction of the “tuned” PYTHIA Monte Carlo (dashed line), described in the text. The acceptance corrected data are integrated over the  $x_F$  interval  $(-0.1, 0.5)$  for  $D_s$  mesons.

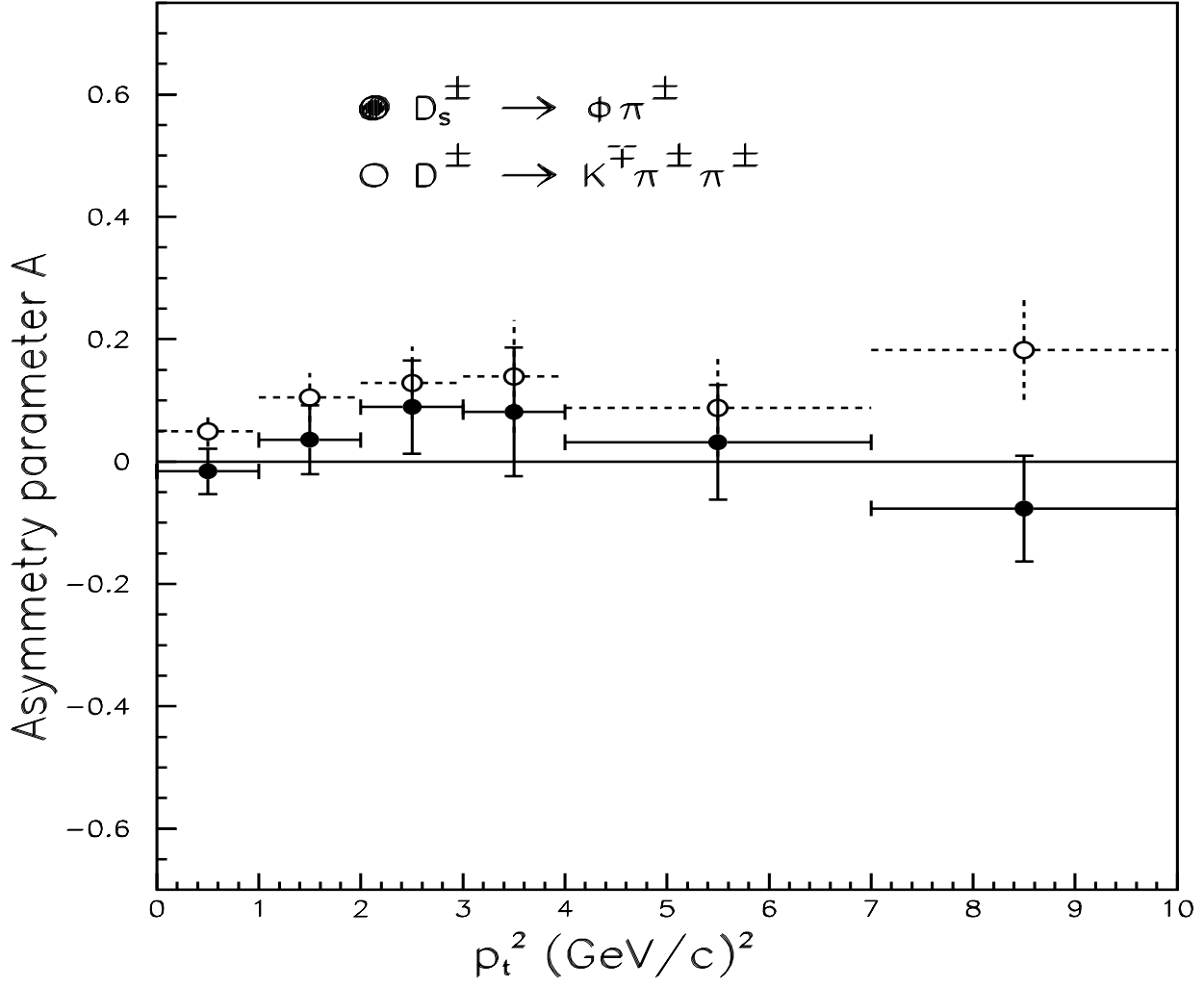


FIG. 5. Comparison of the  $D_s$  (solid circles) and  $D^+$  (open circles) production asymmetries, measured by this experiment, as a function of  $p_t^2$ . The acceptance-corrected data are integrated over the  $x_F$  interval  $(-0.1, 0.5)$  for  $D_s$  mesons and  $(-0.1, 0.8)$  for  $D^\pm$  mesons.